

Comparative Investigation in a Turbine Blade Passage Flows with Several Different Turbulence Models

Mahmood Ebrahimi

Department of Mechanical Engineering,
Iran University of Science and Technology, Tehran, Iran
E-mail: ebrahimi@iust.ac.ir

Mohammad Hossein Roozbahani*

Department of Mechanical Engineering,
Iran University of Science and Technology, Tehran, Iran
E-mail: rozbahani@mecheng.iust.ac.ir

*Corresponding author

Received 15 June 2011; Revised 3 August 2011; Accepted 1 September 2011

Abstract: In the present work a two dimensional numerical investigation of steam flows in a turbine blade passage is performed. A finite volume approach has been used and the pressure-velocity coupling is resolved using the SIMPLE algorithm. The purpose of this paper is to find that one of the used turbulent models is better for this kind of studies. A structured mesh arrangement with boundary layer mesh was adopted to map the flow domain in the blade passage. Pressure profiles around the blades for all models results are compared with the experimental data and good agreement is observed. The three models results of $k-\epsilon$ turbulence models (standard, Realizable and RNG) have compared with Spalart-Allmaras and $k-\omega$ SST models. Based on the results obtained, that all of these models can simulate the flow with reasonable result but the Spalart-Allmaras model and REALIZABLE $k-\epsilon$ model is better than other models with significant in shock capturing. Based on result, Spalart-Allmaras and $k-\omega$ SST models showed a larger boundary layer on suction trailing edge than $k-\epsilon$ models family. Although using REALIZABLE $k-\epsilon$ model leading to savings in computational cost and time.

Keywords: Finite Volume, $k-\epsilon$ Model, $k-\omega$ SST Model, Turbulence Model, Spalart-Allmaras Model, Steam Turbine.

Reference: M. Ebrahimi, M. H. Roozbahani, (1994) 'Comparative Investigation in a Turbine Blade Passage Flows with Several Different Turbulence Models', Majlesi Journal of Mechanical Engineering, Vol. 4/ No.4, pp. 39-45.

Biographical notes: **M. Ebrahimi** received his PhD and MSc in Mechanical Engineering from University of Birmingham, 1995. He is Associate Professor at the Department of Mechanical Engineering, Iran University of Science and Technology, Tehran, Iran. His current research interest includes Experimental and Numerical Simulation of Turbo Machinery. **M. H. Roozbahani** is Graduated Outstanding Student of Mechanical Engineering, Iran University of Science and Technology, Tehran, Iran. He received his BSc. in Aerospace from the Malek-Ashtar University of Technology, Tehran, Iran. His current research focuses on Turbulence Models Applications and Two Phase Fluid Flow Analysis.

1 INTRODUCTION

This paper presents preliminary results of a computational study of turbulent flow in a turbine blade passage. Due to the complex nature of the turbulent flow in a steam turbine, a realistic description of heat transfer mechanism and the corresponding flow physics such as Mach number and pressure variations is still a major concern of the turbomachinery industry. In the literature, there have been a series number of experimental and numerical investigations for flows in steam turbine rotor and/or stator cascades. One of the main concerns of researchers using computational methods is turbulence. This type flow requires a realistic turbulence model. Many researchers have worked on turbo machinery flow with different turbulence model in several characteristics of transonic or supersonic flow. In 1998 Arno Gehrler and Herbert Jericha have studied the External heat transfer predictions for a two-dimensional turbine blade cascade. In their work the Reynolds-averaged Navier-Stokes equations with algebraic (Arnone and Pacciani, 1996), one-equation (Spalart and Allmaras, 1994) and two-equation (low-Re $k-\epsilon$, Biswas and Fukuyama, 1994) turbulence closures are solved with a fully-implicit time-marching finite volume method [1].

In 1999 D.G. Koubogiannis et al. Study the complex flow in a controlled-diffusion compressor cascade at off-design condition with One- and two-equation, low-Reynolds eddy-viscosity turbulence models. Yi Liu in 2005 numerically investigate the transonic viscous flow and heat transfer in a highly loaded turbine blade, where the interaction of a shock wave, a wake and a boundary layer often leads to very complicated flow phenomena. In his works Turbulence is modeled with a low Reynolds number $k-\omega$ model which also considers the compressibility effects [2]. Also S. Djouimaet al. In 2007 studied the turbulence intensities with several two-equation models. Objective of them study is to simulate the transonic gas turbine blade-to-blade compressible fluid flow. In their works experiment performed by Giel and colleagues [3]. Bakhtar et al. did experimental and theoretical study 2-D over rotor-tip cascade turbine blade and got the pressure ratio on the pressure and suction side of the blade and in the middle of the passage between two blades in experimental investigation [4-7]. Their investigation showed that the most important influence of condensation on the pressure distribution is experienced on the suction surface.

At this work the Different turbulence models (Spalart-Allmaras, Standard $k-\epsilon$, RNG $k-\epsilon$, Realizable $k-\epsilon$ and $k-\omega SST$) are used in order to find the most appropriate model to predict the flow around a blade passage

particular in the trailing and leading edges. All simulations done in this work are for stationary and two-dimensional flows.

2 THE EXPERIMENTAL DATA SET AND CASCADE GEOMETRY

Basic geometrical detail of computational domain hasshown in Fig. 1. A structured mesh arrangement with boundary layer mesh was adopted to map the flow domain around the blade. A sketch of the computational setup and the grid is shown in Fig. 2. This grid which gave a high satisfaction (speed convergence and results qualities), was obtained after several attempting improvements concerning upstream and downstream zones.

By increasing the grid numbers and changing the type of arranging mesh, refining, around the blade a proper Y_p value is obtained, and with this value solution results have good agreement with experimental data (Bakhtar et al.) [4,5]. For Enhanced wall treatment the Y_p on the blade edge must be between 1 and 5 and a proper Y_p value is obtained on blade suction face and pressure face, shown as Fig. 3. Conditions to solve the problem are that total pressure, in the inlet boundary is equal to 1.689 bar and temperature is 107.556 degree of Celsius. In outlet boundary condition the static pressure is equal to 0.650 bar.

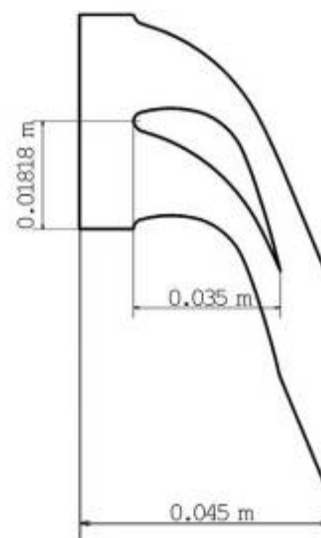


Fig. 1 Geometrical detail of computational domain.

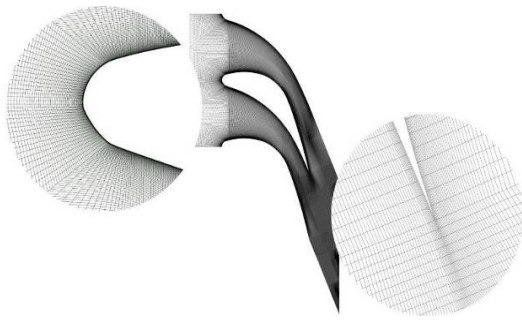


Fig. 2 Structured mesh arrangement

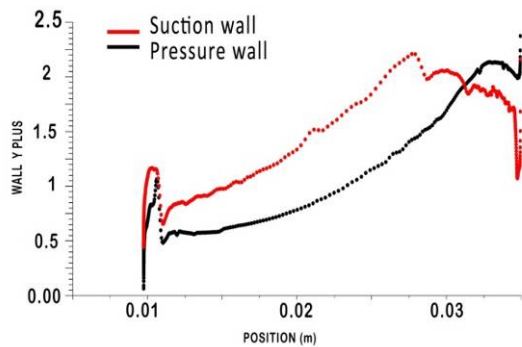


Fig. 3 Y_p on blade suction and pressure face.

3 FLOW SOLVER AND TURBULENCE MODELS

For calculation of viscous flow around a turbine blade passage, a numerical method based on solving equations describing the case under consideration, i.e. RANS equations, is used. These equations have form for the incompressible, steady, two-dimensional flow in Eq. (1). In the Eq. (1), u, v are components of the mean velocity vector, P is the pressure, μ is the viscosity, u', v' are fluctuation parts of the velocity vector, F_1, F_2 are volumetric forces. Furthermore, the model must satisfy the continuity equation, Eq. (2).

$$\rho \left(u \frac{\partial u}{\partial x} + v \frac{\partial u}{\partial y} \right) \rho = F_2 - \frac{\partial p}{\partial y} + \mu \left(\frac{\partial^2 u}{\partial x^2} + \frac{\partial^2 u}{\partial y^2} \right) - \rho \left(\frac{\partial \overline{u'u'}}{\partial x} + \frac{\partial \overline{u'v'}}{\partial y} \right) \quad (1)$$

$$\frac{\partial u}{\partial x} + \frac{\partial u}{\partial y} = 0 \quad (2)$$

The RANS approach calculates statistically averaged (Reynolds-averaged) variables for both steady-state and dynamic flows and simulates turbulence fluctuation effect on the mean flow by using different turbulence models. The steady-state compressible Reynolds-averaged Navier-Stokes equations are solved using a second-order, cell-centered finite-volume scheme on structured grids. The momentum equation is solved sequentially for each component of an intermediate velocity.

4 THE $k-\epsilon$ TURBULENCE MODEL

The standard $k-\epsilon$ turbulence model initially developed by Launder and Spalding [9] is a semi-empirical model based on model transport equations for the turbulent kinetic energy k and its dissipation rate ϵ . The model transport equations for k are derived from the exact equation, while the model transport equation for ϵ is obtained using the physical reasoning and bears little resemblance to its mathematically exact counterpart. In the derivation of the $k-\epsilon$ turbulence model, it is assumed that the flow is highly turbulent, and the effects of the molecular viscosity are negligible. The turbulent kinetic energy k and its rate of dissipation rate ϵ are obtained from transport equations Eq. (3).

$$\begin{aligned} \frac{\partial}{\partial t}(\rho k) + \frac{\partial}{\partial x_i}(\rho k u_i) &= \frac{\partial}{\partial x_j} \left[\left(\mu + \frac{\mu_t}{\sigma_k} \right) \frac{\partial k}{\partial x_j} \right] \\ &+ G_k + G_b - \rho \epsilon - Y_M \\ &+ S_k \end{aligned} \quad (3)$$

$$\begin{aligned} \frac{\partial}{\partial t}(\rho \epsilon) + \frac{\partial}{\partial x_i}(\rho \epsilon u_i) &= \frac{\partial}{\partial x_j} \left[\left(\mu + \frac{\mu_t}{\sigma_\epsilon} \right) \frac{\partial \epsilon}{\partial x_j} \right] \\ &+ \rho C_{1\epsilon} S \epsilon - \rho C_{2\epsilon} \frac{\epsilon^2}{k + \sqrt{\nu \epsilon}} \\ &+ C_{1\epsilon} \frac{\epsilon}{k} C_{2\epsilon} G_b + S_\epsilon \end{aligned}$$

In Eq. (3), μ_t is the eddy viscosity, $C_{1\varepsilon}$ and $C_{2\varepsilon}$ are constants in the sense that they are not changed between calculations. σ_k and σ_ε are the turbulent Prandtl numbers for k and ε respectively. G_k represents the generation of turbulent kinetic energy due to the mean velocity gradients, calculated in a manner consistent with the Boussinesq hypothesis as Eq. 4. Where S is the modulus of the time averaged rate-of-strain tensor, defined as Eq(5). With the time averaged strain rate S_{ij} given by Eq(6). The eddy viscosity in Eq. 6 is computed by combining k and ε as Eq (7), Where C_μ is a constant. In addition to standard model that are explain in above, the Realizable (Shih et al., 1995) and RNG (Yakhot and Orszag, 1986) k - ε model is use in this paper.

$$G_k = \mu_t S^2 \quad (4)$$

$$S = \sqrt{S_{ij} S_{ij}} \quad (5)$$

$$S_{ij} = \frac{1}{2} \left(\frac{\partial \bar{u}_i}{\partial x_j} + \frac{\partial \bar{u}_j}{\partial x_i} \right) \quad (6)$$

$$\mu_t = \rho C_\mu \frac{k^2}{\varepsilon} \quad (7)$$

5 THE SPALART-ALLMARAS TURBULENCE MODEL

The model of Spalart and Allmaras (1992) exhibits good convergence properties and has a remarkably accurate response to pressure gradient. It consists of one transport equation for a modified eddy-viscosity, $\tilde{\nu}$, Eq(8). In which the source term Q , earn from Eq(9).

$$\bar{u} \cdot \text{grad } \tilde{\nu} = \frac{1}{C_{b3}} [\text{div}((\nu + \tilde{\nu}) \text{grad } \tilde{\nu}) + C_{b2} (\text{grad } \tilde{\nu} \cdot \text{grad } \tilde{\nu}) + Q] \quad (8)$$

$$Q = C_{b1} (1 - f_{t2}) \tilde{S} \tilde{\nu} + \left(\frac{C_{b1}}{k^2} f_{t2} - C_{w1} f_w \right) \left(\frac{\tilde{\nu}}{d} \right)^2 \quad (9)$$

The eddy viscosity in this model is equal to Eq(10).

$$\mu_t = \rho \tilde{\nu} f_{v1} \quad (10)$$

The model damping functions, auxiliary relations and trip term are defined as Eq(11), Eq(12) and Eq(13). In which d is the distance to the nearest wall, k the von Karman constant and \tilde{S} the vorticity expressed in terms of the rotation tensor, Eq(14). Finally, the model closure coefficients are equal to Eq(15) and Eq(16). The wall boundary condition is in Eq(17).

$$f_{v1} = \frac{x^3}{x^3 + C_{v1}^3}, f_{v2} = 1 - \frac{x}{1 + x f_{v1}}, \quad x = \frac{\tilde{\nu}}{\nu} \quad (11)$$

$$f_w = g \left[\frac{1 + C_{w3}^6}{g^6 + C_{w3}^6} \right]^{\frac{1}{6}}, \quad g = r + C_{w2}(r^6 - r), \quad r = \frac{\tilde{\nu}}{\tilde{S} k^2 d^2} \quad (12)$$

$$\tilde{S} = S + \frac{\tilde{\nu}}{k^2 d^2} f_{v2}, \quad S = \sqrt{2 \Omega_{ij} \Omega_{ij}} \quad (13)$$

$$f_{t2} = C_{t3} \exp(-C_{t4} x^2), \quad \Omega_{ij} = \frac{1}{2} \left(\frac{\partial u_i}{\partial x_j} - \frac{\partial u_j}{\partial x_i} \right) \quad (14)$$

$$[c_{b1} = 0.1355, c_{b2} = 0.622, c_{b3} = 2/3, c_{v1} = 7.1] \quad (15)$$

$$C_{w1} = (C_{b1}/k^2) + ((1 + C_{b2})/C_{b3}), \quad C_{w2} = 0.3, C_{w3} = 2, C_{t3} = 1.2, C_{t4} = 0.5 \quad (16)$$

$$\tilde{\nu}_t = 0 \quad (17)$$

6 THE K- ω SST TURBULENCE MODEL

The shear-stress transport (SST) k - ω model was developed by Menter [8] to effectively blend the robust and accurate formulation of the k - ω model in the near-wall region with the free-stream independence of the k - ε model in the far field. To achieve this, the k - ε model is converted into ak - ω model formulation. The k - ω SST model is similar to the standard k - ω model, but the definition of the turbulent viscosity is modified to

account for the transport of the turbulent shear stress and the modeling constants are different. The k - ω SST model has a similar form to the standard k - ω model, Eq(18).

$$\frac{\partial}{\partial t}(\rho k) + \frac{\partial}{\partial x_i}(\rho k u_i) = \frac{\partial}{\partial x_j} \left(\Gamma_k \frac{\partial k}{\partial x_j} \right) + \tilde{G}_k - Y_k + S_k \quad (18)$$

$$\begin{aligned} \frac{\partial}{\partial t}(\rho \omega) + \frac{\partial}{\partial x_i}(\rho \omega u_i) \\ = \frac{\partial}{\partial x_j} \left(\Gamma_\omega \frac{\partial \omega}{\partial x_j} \right) + \tilde{G}_\omega - Y_\omega + S_\omega \end{aligned}$$

In these equations, \tilde{G}_k represents the generation of turbulence kinetic energy due to mean velocity gradients. \tilde{G}_ω represents the generation of ω . Γ_k and Γ_ω represent the effective diffusivity of k and ω . Y_k and Y_ω represent the dissipation of k and ω due to turbulence. D_ω represents the cross-diffusion term. S_k and S_ω are user-defined source terms that are equal to zero at this work.

The effective diffusivities for the SST k - ω model are given by Eq(19) and Eq(20).

$$\Gamma_k = \mu + \frac{\mu_t}{\sigma_k} \quad (19)$$

$$\Gamma_\omega = \mu + \frac{\mu_t}{\sigma_\omega} \quad (20)$$

Where σ_k and σ_ω are the turbulent Prandtl numbers for k and ω , respectively. The turbulent viscosity, μ_t , is computed as Eq(21).

$$\mu_t = \frac{\rho k}{\omega} \frac{1}{\max \left[\frac{1}{\alpha^*}, \frac{SF_2}{\alpha_1 \omega} \right]} \quad (21)$$

7 WALL TREATMENT

This section focuses on the near-wall behavior of the turbulence models presented above, in particular on the treatment of the wall boundary condition in the

framework of the immersed boundary. The modified eddy viscosity is zero at the wall and it has the property of varying in a nearly linear fashion from the wall throughout the law-of-the-wall layer thus decreasing the sensitivity to grid resolution and wall clustering (Durbin and PetterssonReif (2001))[9]. The application of wall functions to modeling the near-wall region may significantly reduce both the processing and storage requirements of a numerical model, while producing an acceptable degree of accuracy. The non-dimensional wall parameter is defined as Eq(22).

$$y_p = \frac{\rho \sqrt{\frac{\tau_w}{\rho_w}} y_p}{\mu} \quad (22)$$

In Eq(22), y_p is the distance from the first computational node to the wall and the subscript w denotes wall properties, "Speziale, Abid, Anderson et al. [10]". The standard wall functions are based on the proposal of Launder and Spalding (1974), and have been widely used for industrial flow. Kim and Choudhury (1995) proposed the use of the non-equilibrium wall functions in order to improve the accuracy of the standard wall functions. The key elements in non-equilibrium wall functions are pressure-gradient sensitized Launder and Spalding (1974) log-law for mean velocity and the two layer-based concept to compute the turbulence kinetic energy in the wall-adjacent cells. In the two-layer model, the whole domain is subdivided into a viscosity affected region and a fully-turbulent region. The one equation model of Wolfstein (1969) is employed in the viscosity-affected region [11].

Enhanced wall treatment that is used at presented paper is a method of near-wall modelling that utilizes the combination of a two-layer zonal model with enhanced wall functions. If the mesh is fine enough to resolve the laminar sub layer within the order of $Y_p \approx 1$, then the wall treatment is identical to the two-layer zonal model, however, this mesh requirement can place significant demands on computational processing and storage infrastructure [12].

8 RESULTS AND DISCUSSION

The result of pressure ratio on pressure and suction surfaces from simulation is compared with experimental data in Fig. 4. Good agreements have been seen between simulation models computations and experimental data. As can be seen in Fig. 4,

Turbulence models, from a distance of 0.03 to the end of Blade, differ with each other, Where the end shock of high Blade, to treat with low Blade wall suction. The investigated models have similar behaviour, but in the shock zone these behaviours will be different. Different turbulence models utilized, in different number of iterations, to achieve the desired response. The number of iterations for convergence of each method is given in Table 1.

Table 1 Model convergence iterations number

Turbulence modal name	Iterations number
Standard k-ε	764
RNG k-ε	562
Realizable k-ε	410
k-ω sst	1050
Spalart-Allmaras	2751

The Realizable and Spalart-Allmaras model calculate the Mach and pressure contour in domain better than RNG and Standard model well be seen in Figs. 5&.6. Although Spalart-Allmaras and Realizable model both have captured the shock their like, but Spalart-Allmaras has solved with the 2751 iterations and Realizable with the 410 iterations. In this investigation the flow was superheated and there is any nucleating. So when the two-phase nucleating flow must be solved, the model should be used which is faster in computations because the nucleating flow equations solution, requires a lot of time and high CPU terms. Velocity vectors on the blade trailing edge for all tests are shown in Fig. 7.

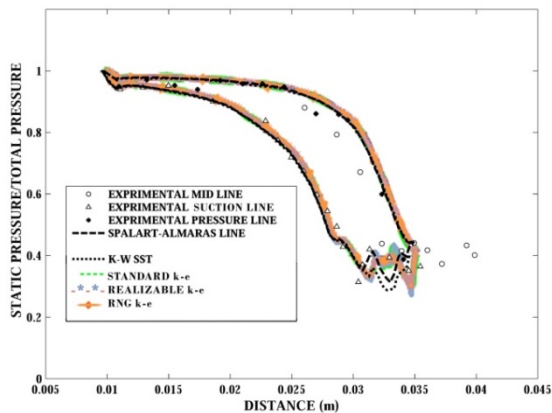


Fig. 4 Comparison between simulation and experimental results for pressure ratio on pressure and suction surfaces $P_{t1}=1.689 \text{ bar}, T_0=107.556 \text{ }^\circ\text{C}, P_{02}=0.650 \text{ bar}.$

As shown in Fig. 7 the Spalart-Allmaras and k-ω SST models showed a larger boundary layer on suction trailing edge than k-ε models family. The velocity profile for Spalart-Allmaras and k-ω SST models has a sharp slope.

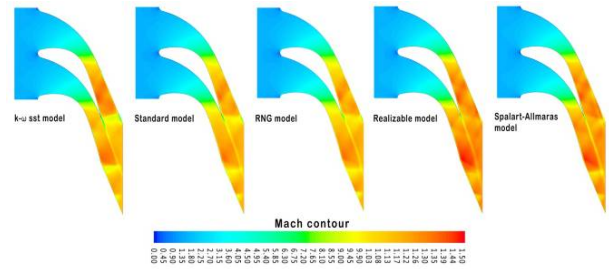


Fig. 5 Comparison of Mach number contours in the passage between blades for different turbulence models $P_{t1}=1.689 \text{ bar}, T_0=107.556 \text{ }^\circ\text{C}, P_{02}=0.650 \text{ bar}.$

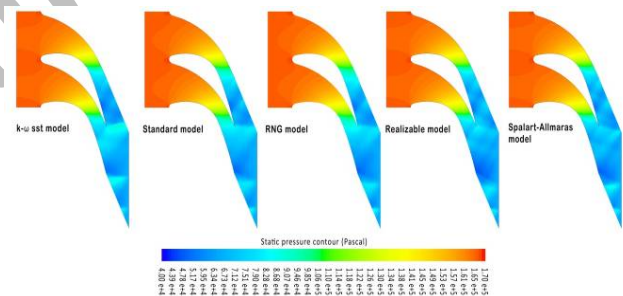


Fig. 6 Comparison of static pressure contours in the passage between blades for different turbulence models $P_{t1}=1.689 \text{ bar}, T_0=107.556 \text{ }^\circ\text{C}, P_{02}=0.650 \text{ bar}.$

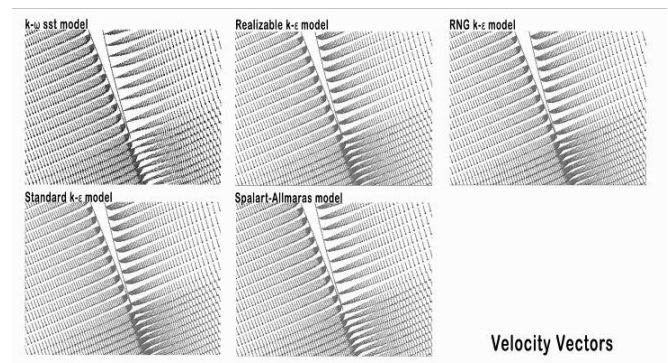


Fig. 7 Velocity vectors for all turbulence models.

8 CONCLUSION

- The RANS solver is applied to turbulent flow inside the turbine blade passage with two different turbulence models. Numerical simulations were made to determine the flow characteristics and mainly the pressure distribution around a turbine blade.

- The development of shock on the suction surface for each simulation is successfully reproduced by the present turbulence models. Much effort was invested in the grid in order to provide quality results.

- Several turbulence models were compared in order to determine which the most appropriate model to predict this flow is.

- Since our simulations show that all models give good results compared with experiment but for shock capturing the Realizable $k-\varepsilon$ and Spalart-Allmaras have been better than others models and Spalart-Allmaras and $k-\omega$ SST models showed a larger boundary layer on suction trailing edge than $k-\varepsilon$ models family.

- The Realizable model compare to Spalart-Allmaras can save the time and CPU cost consuming in this kind of investigations. So far instead of using all these models to determine the effects of nucleation conditions in future works only the Realizable $k-\varepsilon$ model is selected.

REFERENCES

- [1] Gehrler, A. and Jericha, H., "External Heat Transfer Predictions in a Highly-Loaded Transonic Linear Turbine Guide Vane Cascade Using an Upwind Biased Navier-Stokes Solver," ASME Paper 98-GT-238, 1998.
- [2] Liu, Y. "Aerodynamics and Heat Transfer Predictions in a Highly Loaded Turbine Blade," International Journal of Heat and Fluid Flow 28, 2007.
- [3] Djouimaa, S. Messaoudi, L. and Paul W. Giel, "Transonic Turbine Blade Loading Calculations Using Different Turbulence Models – Effects of Reflecting and Non-Reflecting Boundary Conditions," Applied Thermal Engineering 27, 2007, pp. 779–787.
- [4] Bakhtar, F., Shojaee-Fard, M. H., and Savage, R. A. "An Investigation of Nucleating Flows of Steam in a Cascade of Turbine Blading-Effect of Overall Pressure Ratios," In Proceedings of ASME Fluids Engineering Conference on Cavitation and Multiphase Flow Forum (Ed. D. Furuya), Vol. FED 153, 1993, pp. 205-208.
- [5] Bakhtar, F., Webb, R. A., Shojaee-Fard, M. H., and Savage, R. A., "An Investigation of Nucleating Flows of Steam in a Cascade of Blading-Effect of Overall Pressure Ratios," In Proceedings of Cavitation and Multiphase Flow Forum (Ed. O. Foruya), ASME Fluids Engineering Conference, Washington DC, FED Vol. 153, 1993, pp. 205-208.
- [6] Bakhtar, F., Ebrahimi, M. and Bamkole, B. O. "On the Performance of a Cascade of Turbine Rotor Tip Section Blading in Nucleating Steam. Part 2: Wake Traverses," Proc. Instn Mech. Engrs, Part C: J. Mechanical Engineering Science, 209(C3), 1995, pp. 167-177.
- [7] Bakhtar, F., Ebrahimi, M. and Webb, R.A. "On the Performance of a Cascade of Turbine Rotor Tip Section Blading in Nucleating Steam, Part 1: Surface Pressure Distributions," Proc. Inst. Mech. Eng. C209, 1995.
- [8] Menter, F.R. "Two-Equation Eddy-Viscosity Turbulence Models for Engineering Applications," AIAA Journal, Vol. 32, No. 8, 1994, pp. 1598-1605.
- [9] Durbin, P. A. and Pettersson-Reif, B. A. "Statistical Theory and Modeling for Turbulent Flows," Wiley, New York, 2001.
- [10] Speziale, C.G., Abid, R. and Anderson, E.C. "Critical Evaluation of Two-Equation Models for Near-Wall Turbulence," AIAA J., Vol. 30 No. 2, 1992, pp. 324-331.
- [11] Nicholas, J. Chen Mulvany, Li., Tujiyuan, Y. and Anderson, B. "Steady-State Evaluation of 'Two - Equation' RANS (Reynolds-averaged Navier-Stokes) Turbulence Models for High-Reynolds Number Hydrodynamic Flow Simulations," Maritime Platforms Division, DSTO-TR-1564.
- [12] Chun, H.H. Chang, R. H. "Turbulence Flow Simulation for Wings in Ground Effect with Two Ground Condition Fixed and Moving Ground," International Journal of Maritime Engineering, 2003.
- [13] Spalart, P. R. and Allmarat, S. R., "A One Equation Turbulence Model for Aerodynamic Flows, La Recherche Aerospatiale," No.1, 1994, pp 5-21.
- [14] Spalart, P. R. and Allmarat, S. R., "A One Equation Turbulence Model for Aerodynamic Flows, La Recherche Aerospatiale," No.1, pp 5-21
- [15] AndChesse, S., "Optimal Dynamics of Actuated Kinematic Chains, Part 2: Problem Statements and Computational Aspects," European Journal of Mechanics A/Solids, Vol. 24, 2005, pp. 472–490.
- [16] Bertolazzi, E., Biral, F. and Da Lio, M., "Symbolic-Numeric Indirect Method for Solving Optimal Control Problems for Large Multibody Systems," Multibody System Dynamics, Vol. 13, No. 2, 2005, pp. 233-252.
- [17] Callies, R. and Rentrop, P., "Optimal Control of Rigid-Link Manipulators by Indirect Methods," GAMM-Mitt., Vol. 31, No. 1, 2008, pp. 27 – 58.
- [18] Mohri, A., Furuno, S. and Yamamoto, M., "Trajectory Planning of Mobile Manipulator with End-Effector's Specified Path," Proc. IEEE Int. Conf. on Intelligent Robots and systems, 2001, pp. 2264-2269.